Developmental Biology 343 (2010) 124–137

Contents lists available at ScienceDirect

Developmental Biology

journal homepage: www.elsevier.com/developmentalbiology

Evolution of Developmental Control Mechanisms

Developmental expression of a molluscan RXR and evidence for its novel, nongenomic role in growth cone guidance

Christopher J. Carter, Nathan Farrar, Robert L. Carlone, Gaynor E. Spencer *

Dept. Biological Sciences, Brock University, 500 Glenridge Ave. St. Catharines, Ontario, Canada L2S 3A1

ARTICLE INFO

Article history:
Received for publication 29 October 2009
Revised 10 March 2010
Accepted 25 March 2010
Available online 8 April 2010

Keywords:
Retinoic acid
Lymnaea stagnalis
Retinoids
Growth cone
Chemotropism
Neurites
Molluscan development
9-cis RA

ABSTRACT

It is well known that the vitamin A metabolite, retinoic acid, plays an important role in vertebrate development and regeneration. We have previously shown that the effects of RA in mediating neurite outgrowth, are conserved between vertebrates and invertebrates (Dmetrichuk et al., 2005, 2006) and that RA can induce growth cone turning in regenerating molluscan neurons (Farrar et al., 2009). In this study, we have cloned a retinoid receptor from the mollusc *Lymnaea stagnalis* (*Lym*RXR) that shares about 80% amino acid identity with the vertebrate RXRα. We demonstrate using Western blot analysis that the *Lym*RXR is present in the developing *Lymnaea* embryo and that treatment of embryos with the putative RXR ligand, *9-cis* RA, or a RXR pan-agonist, PA024, significantly disrupts embryogenesis. We also demonstrate cytoplasmic localization of *Lym*RXR in adult central neurons, with a strong localization in the neuritic (or axonal) domains. Using regenerating cultured motor neurons, we show that *Lym*RXR is also present in the growth cones and that application of a RXR pan-agonist produces growth cone turning in isolated neurites (in the absence of the cell body and nucleus). These data support a role for RXR in growth cone guidance and are the first studies to suggest a nongenomic action for RXR in the nervous system.

Introduction

Retinoic acid (RA) is the active metabolite of vitamin A and is well known to influence morphogenesis during vertebrate development (Maden and Hind, 2003; Maden, 2007). It can also act as a trophic factor and has been implicated in neurite outgrowth (Corcoran et al., 2000; Maden et al., 1998; Wuarin et al., 1990) and regeneration (Dmetrichuk et al., 2005) of the nervous system. Retinoic acid classically acts through nuclear receptors that act as transcription factors to affect downstream activation of various genes, including neurotrophins, cytokines, cell surface molecules (reviewed in Gudas, 1994; Mey and McCaffery, 2004), as well as specific genes involved in neurite outgrowth, such as *NEDD9* (Knutson and Clagett-Dame, 2008) and *neuron navigator 2* (Muley et al., 2008). The nuclear receptors responsive to RA include the retinoic acid receptors (RARs) and the retinoid X receptors (RXRs), and at least three classes of each have been identified (α, β, and γ). RARs bind both *all-trans* and *9-cis* RA isomers, whereas the RXRs (at least in vertebrates) bind only *9-cis* RA (Heyman et al., 1992). There is evidence that both RARs and RXRs play a role in neurite outgrowth and/or neurite regeneration; RARβ plays a major role in the induction of neurite outgrowth from both embryonic (Corcoran et al., 2000) and adult (Dmetrichuk et al., 2005) spinal cord neurons, while RXR has been suggested to play a role in motor neuron innervation of limbs in mice (Solomin et al., 1998). Both RARs and RXRs are found in vertebrate nervous systems, but until recently, it was generally believed that nonchordates possessed only RXRs. However, evidence for putative RARs has now emerged from EST/genomic databases in annelids and molluscs (Albalat and Canestro, 2009), and a molluscan RAR has now been cloned (Carter and Spencer, 2009; accession no. GU932671).

It has become increasingly evident that many effects of retinoic acid are conserved between vertebrate and invertebrate species. The presence of RA in invertebrates has been implicated by the presence of retinoic acid binding proteins in the insect (Mansfield et al., 1998), shrimp (Gu et al., 2002), and marine sponge (Biesalski et al., 1992). RA has also been detected in fiddler crab limb blastemas (Chung et al., 1998) and in the locust embryo (Nowickyj et al., 2008), suggesting a role in both limb regeneration and embryonic development. More recently, we have shown for the first time that RA is present in the invertebrate CNS (Dmetrichuk et al., 2008) and demonstrated that (in the absence of other neurotrophic factors) it induces neurite outgrowth as well as growth cone turning in cultured neurons of the mollusc, *Lymnaea stagnalis* (Dmetrichuk et al., 2006, 2008; Farrar et al., 2009). The mechanisms underlying the neurotrophic and chemotropic effects of retinoic acid in *Lymnaea* are, at present, largely unknown, although we have recently shown that the RA-induced growth cone turning involves a nongenomic mechanism that requires protein synthesis and calcium influx (Farrar et al., 2009).

In this study, we have cloned a RXR from the CNS of *Lymnaea* that demonstrates a high sequence homology with the vertebrate RXRα.

* Corresponding author. Fax: +1 905 688 1855.
E-mail address: gspencer@brocku.ca (G.E. Spencer).

0012-1606/$ – see front matter © 2010 Elsevier Inc. All rights reserved.
doi:10.1016/j.ydbio.2010.03.023

Our aim was then to determine whether this *Lymnaea* RXR plays a role in either embryonic development and/or neuronal regeneration of central neurons in *L. stagnalis*.

Materials and methods

Cloning of L. stagnalis RXR

L. stagnalis used in this study were laboratory-bred and kept in aerated, artificial pond water and fed lettuce and NutraFin Max Spirulina fish food (Hagen). RT–PCR was performed on cDNA generated from total RNA extracted from the *Lymnaea* CNS. Briefly, reverse transcription was carried out with a mixture of poly A and random hexamer primers according to the iScript cDNA synthesis kit (BioRad). cDNA was then amplified with 40 pmol of forward (5′-CGA CAA AAG ACA GAG AAA CAG ATG YCA RTA YTG-3′) and reverse (5′-GTC TCT GAA GTG TGG GAT TCT TTT NGC CCA YTC-3′) degenerate primers. After 3 min of denaturation at 95 °C, 35 cycles at 95 °C for 30 sec, annealing at 55 °C for 30 sec, and elongation at 72 °C for 1 min were performed with an Eppendorf Mastercycler Personal Thermocycler. Analysis of the product was carried out on 1% agarose gels in TAE buffer stained with ethidium bromide. Fragments of interest were excised from the gel and cloned into the pGemTEasy vector system (Promega). Sequencing was performed by GénomeQuébec (Montréal, Canada) using 3730xl DNA Analyzer systems from Applied Biosystems. Full-length cDNA was obtained by performing multiple rounds of 5′ and 3′ RACE with cDNA prepared from the same *Lymnaea* CNS preparations with the SMART RACE cDNA amplification kit (Clontech).

Antibodies

We designed antibodies against a synthetic peptide from the predicted 'hinge' region of the *Lymnaea* RXR covering the amino acid residues 183–198 between the DNA binding domain (DBD) and ligand binding domain (LBD). This custom-made *Lym*RXR antibody was produced in New Zealand white rabbits and affinity-purified from the antisera by Pacific Immunology Corp. (Ramone, CA, USA). In some Western blotting procedures, a commercial antibody against human GAPDH (Abcam Inc.) was used as a cytosolic fraction marker, and a commercial antibody against human actin (Sigma-Aldrich) was used as a control.

Lymnaea embryos

To investigate *Lym*RXR protein levels during *Lymnaea* development, egg masses were first incubated in pond water at room temperature and allowed to reach various stages of development, as described in Nagy and Elekes (2000). These stages included day 0 of embryogenesis (when egg mass is first laid and before first cleavage), the trochophore stage (approx. 36–60 h of embryogenesis), the veliger stage (approx. 60–96 h of embryogenesis), the adult-like stage just before hatching (96–192 h of embryogenesis), and hatchlings. When the embryos reached the desired stage, the capsules were removed from their gelatinous surroundings, total protein was extracted, and Western blotting was performed according to the protocol listed below for adult CNSs. These experiments were performed twice.

To determine if *Lym*RXR plays a role in *Lymnaea* development, embryos were incubated in a synthetic RXR agonist (PA024, a kind gift from Dr. H. Kagechika, Tokyo) and *9-cis* RA (Sigma-Aldrich). At day 0 of embryogenesis (when egg mass is first laid), capsules were teased out of the gelatinous surroundings in which they were embedded and maintained in pond water at room temperature for 30 h (until the end of the gastrulation stage). This separation of the capsules increased probability of penetration of the agonist PA024 and *9-cis* RA while still allowing normal development of the egg inside the capsule (Creton et al., 1993). The RXR agonist PA024 (10^{-7} M), *9-cis* RA (10^{-7} M), or DMSO (0.001%, vehicle control) was added to separate dishes of embryos at 30 h of embryogenesis (this was previously shown to be the most sensitive stage to disruption by RA; Creton et al., 1993). At days 6–7 of embryogenesis, embryos showing eye and/or shell malformations, or arrested development at the trochophore stage, were scored and compared with the DMSO control embryos. These experiments were also performed twice with incubation of embryos in RXR antagonists alone (PA452 = 10^{-6} M and HX531 = 10^{-6} M both a kind gift from Dr. H. Kagechika, Tokyo) in the exact same manner as described above. Statistical analysis was composed of multiple Fisher exact tests that were then Bonferroni–Holm-corrected.

Western blotting

To investigate the expression of *Lym*RXR protein, the adult *Lymnaea* CNS (or whole embryos) were homogenized in lysis buffer containing 150 mM NaCl, 50 mM Tris–HCl (pH 7.5), 10 mM EDTA, 1% Trition X-100, 1 mM PMSF, and 0.01% Protease Inhibitor Cocktail (Sigma-Aldrich) with a PowerGen handheld homogenizer (Fisher Scientific). The homogenates were centrifuged 20,000 × *g* at 4 °C for 30 min. Fifteen micrograms of protein from each extract was separated on a discontinuous SDS–polyacrylamide gel (12% resolving and 4% stacking) and electroblotted onto a nitrocellulose membrane (BioRad). For embryo experiments, gels were electrophoresed in duplicate under identical conditions; one was stained with Coomassie blue to ensure equal loading of protein and the other was subjected to Western blot analysis. The membranes were washed for 5 min in 1× PBS and then blocked in 1× PBS/0.1% Tween-20 (PBT) with 3% skim milk powder (wt./vol.) for 1 h. The membranes were then incubated with affinity purified *Lymnaea* RXR antibody at a dilution of 1:2500 in PBT/3% skim milk overnight at 4 °C with gentle horizontal shaking. This was followed by 4 × 5 min washes at room temperature in PBT and incubation with a 1:15,000 dilution of Alexa Fluor 680 goat antirabbit secondary antibody (Invitrogen). After 4 × 5 min washes in PBT and one wash in 1× PBS, the membranes were imaged with the LI-COR Odyssey Infrared Imaging System at a wavelength of 700 nm.

To investigate the subcellular expression of *Lym*RXR in the *Lymnaea* CNS, as well as in embryos just before hatching, total proteins from the cytoplasmic, membrane, and nuclear compartments were isolated according to directions from the Qproteome Cell Compartment kit (Qiagen). These protein fractions were loaded onto a discontinuous SDS–polyacrylamide gel, and *Lym*RXR was detected by Western blotting technique as previously described above. Anti-GAPDH (Abcam Inc.) was used as a cytosolic fraction marker, and successful isolation of protein from all three compartments of the CNS was confirmed by staining for actin. These experiments were performed twice for embryos and four times for the adult CNS.

Immunostaining

For immunostaining, the CNSs isolated from the snails were fixed in 4% paraformaldehyde in PBS at 4 °C overnight and washed in 10% sucrose/PBS for 2 h, 20% sucrose/PBS for 2 h, and then 30% sucrose/PBS overnight at 4 °C. After embedding the fixed CNSs in Optimal Cutting Temperature (OCT) Compound (Tissue-Tek), serial 20 µm sections were cut using a cryostat (Leica Microsystems) and placed on SuperFrost Plus slides (Fisher Scientific). For immunostaining of cultured neurons following outgrowth (24–36 h), cells were fixed in 4% paraformaldehyde in PBS at 4 °C overnight. From this point on, all immunostaining procedures were the same for CNSs and cultured neurons. The samples were washed in PBS and then permeabilized in 0.3% Triton X-100 in PBS (PBT) for 20 min and blocked in 5% normal goat serum (NGS) in PBT for 1 h at room temperature. The samples were then incubated with the primary *Lym*RXR antibody diluted 1:100 in blocking solution at 4 °C overnight. As a control, preparations

were also incubated only in blocking solution, without the primary antibody, at 4 °C overnight. All samples were then washed in PBT 3×5 min and incubated in 1:500 dilution of Alexa Fluor 488 goat antirabbit secondary antibody (Invitrogen) in blocking buffer at room temperature for 2 h. The samples were washed in 3×5 min in PBT and counterstained with DAPI for 2 min to visualize the nuclei. After a brief wash in PBS, the specimens were coverslipped with antifade Fluorosave mounting media (Calbiochem).

Cell culture procedures

All cell culture procedures were performed as described previously (Dmetrichuk et al., 2006; Farrar et al., 2009; Ridgway et al., 1991). Briefly, under sterile conditions, the central ring ganglia were isolated, subjected to a number of antibiotic washes and enzymatic treatment, and then pinned down in a dissection dish and bathed in high osmolarity (L-15 derived) defined medium (DM; Ridgway et al., 1991). Using a pair of fine forceps, the connective tissue sheath surrounding the ganglia was removed, and identified Pedal A (PeA) motor neurons were individually extracted using gentle suction applied via a fire-polished pipette attached to a microsyringe. The individually identified PeA somata were plated directly on poly-L-lysine-coated dishes (onto a glass coverslip) containing brain-conditioned medium (CM; Wong et al., 1981) and *at*RA (10^{-7} M) to promote outgrowth. Cells were maintained in the dark at 22 °C overnight. An inverted microscope (Zeiss Axiovert 200) was used for all phase and fluorescent imaging of cultured cells.

Growth cone assays

Growth cone assays were performed in an identical manner to those described in detail elsewhere (Farrar et al., 2009). Briefly, a pressure pipette (Eppendorf-Femtojet; 4–8 µm) containing *9-cis* RA (10^{-5} M), or the RXR agonist, PA024 (10^{-5} M or 10^{-6} M), was positioned 50 to 100 µm from an actively growing growth cone. Pressures between 5 and 12 hPa were used to apply the agonists, while holding pressures of 1–2 hPa were used during rest periods to prevent backflow of bath solution. Concentrations detected at the growth cone were likely 100–1000 times less than those present in the pipette (Lohof et al., 1992). Control experiments using the DMSO vehicle solution for the agonist (0.1%) were performed in the exact same manner. For isolated growth cone experiments, neurites were mechanically separated from the cell body using a sharp glass electrode (Farrar et al., 2009). To test whether the RXR agonist-induced turning was inhibited in the presence of RXR antagonists, PA024 was applied to the growth cones, either in the presence of bath-applied DMSO vehicle control (final bath concentration of 0.01%) or in the presence of the RXR antagonist PA452 (final bath concentration of 10^{-6} M) or HX531 (final bath concentration of 10^{-6} M).

Growth cone behaviour in both intact and isolated neurites in response to drug application was monitored for at least 1 h, and the maximum turning angle was recorded. A one-way analysis of variance (1-way ANOVA) was performed on growth cone data sets, and a Tukey–Kramer *post hoc* test was used to determine statistical significance. Results are expressed as mean ± standard error of the mean (SEM) and are deemed significant when $P<0.05$.

Results

Sequencing of LymRXR

Using RT–PCR with degenerate primers designed from other known RXR sequences, we obtained an initial cDNA fragment from the CNS of *L. stagnalis*. A full-length RXR cDNA was elucidated by multiple rounds of 5′ and 3′ RACE from the initial cDNA clone. The final full-length cDNA we obtained was 1593 bp, with a 1308 bp major open reading frame that encodes for a 436 aa RXR protein (we termed *Lym*RXR; accession no. AY846875). This *Lym*RXR has an overall amino acid identity of 97% with the RXR from a closely related mollusc, *Biomphalaria glabrata* (*Bg*RXR; accession no. AAL86461). Of the various vertebrate RXR subtypes, *Lym*RXR is most similar to the RXRα subtype. The predicted DNA-binding domain (DBD) of *Lym*RXR shares ~89% amino acid identity with the *Rattus norvegicus* RXRα (accession no. NP_036937), while the predicted ligand-binding domain (LBD) shares ~81% amino acid identity with rat RXRα (Fig. 1).

LymRXR in the developing embryo

RA, acting as a transcriptional activator, is well known to play a role in vertebrate development. Our first aim following the identification of *Lym*RXR was thus to determine whether the RXR protein was present in the developing *Lymnaea* embryo. *Lymnaea* embryogenesis is intracapsular, lasting about 8 days in total. There are three major developmental stages, defined as the trochophore stage (approx. 36–60 h of embryogenesis), veliger stage (60–96 h of embryogenesis), and the postmetamorphic stage (96 h to hatching). It is during the veliger stage where ganglia are first detected (Nagy and Elekes, 2000) and many of the organs begin to develop (Meshcheryakov, 1972). Following hatching at about 8 days, the animal starts its juvenile, free-living existence.

A custom-made antibody against a synthetic peptide from the 'hinge' region between the DBD and LBD was used to detect the *Lym*RXR protein during the various stages of embryogenesis. Western blot analysis of *Lymnaea* embryo total protein revealed a band of approximately 47 kDa in size, close to the predicted molecular weight of 48 kDa (Fig. 2A). *Lym*RXR protein was present as early as the trochophore stage (approx. 36–60 h) and was present in all subsequent stages studied, with its expression appearing maximal at the hatchling stage (Fig. 2A). RXR is typically known for its role as a nuclear hormone receptor and transcription factor. Thus, to determine its nuclear localization in cells of the *Lymnaea* embryo, total protein fractions were isolated from the cytoplasm, membrane, and nucleus of embryos, immediately before hatching, using a Qproteome Cell Compartment kit (Qiagen). Western blot analysis showed a positive signal for RXR not only in the nuclear compartment of embryos but also in the cytoplasmic and membrane compartments (Fig. 2B).

It is well documented that disruptions of RA signaling in vertebrates, either by inhibition of its synthesis or by exogenous addition of RA, can lead to a wide array of developmental defects in limb, CNS, and main body axis formation (Durston et al., 1989; Sive et al., 1990; Stratford et al., 1996). Creton et al. (1993) have also previously shown that RA disrupted embryogenesis in *Lymnaea*, mainly by affecting eye and shell development. Having determined that RXR is present in the embryo, we next aimed to determine whether known RXR agonists/ligands would disrupt the normal pattern of development in *Lymnaea*. We also used eye and shell formation as indicators of normal growth because these are easily visualized and characterized using light microscopy, shortly after the veliger stage. Eyes normally become pigmented at the end of the veliger stage (at about 96 h), and the shell extends over the visceral masses just a few hours later (Nagy and Elekes, 2000).

Lymnaea embryos were maintained within their capsules but were removed from their gelatinous surroundings. Capsuled embryos were treated with a synthetic RXR pan-agonist, PA024 (10^{-7} M; $n=40$), the putative RXR ligand, *9-cis* RA (10^{-7} M; $n=40$), and DMSO as the vehicle control (0.001%; $n=40$). These treatments were started at the gastrula stage (30 h) and continued for the next 5 days of embryonic development. In the presence of DMSO, both shell (Fig. 2C) and eye (Figs. 2C and Di) development appeared normal. However, we found that treatments with *9-cis* RA and PA024 produced defects in both eye (Figs. 2Dii–iii and G) and shell formation (Figs. 2E and H) in a significant number of embryos. Eye defects included either missing

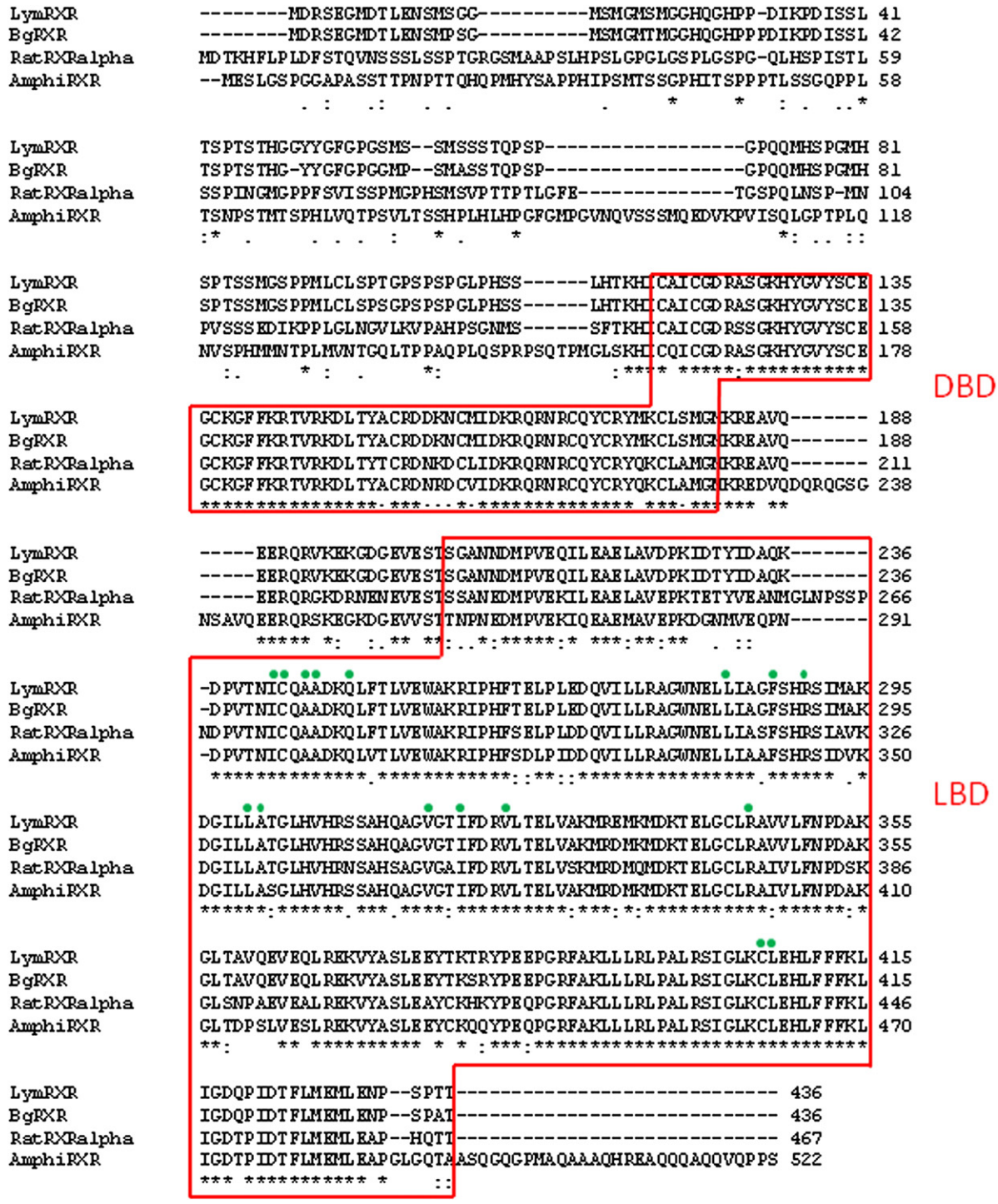

Fig. 1. The *Lymnaea* RXR sequence. Multiple sequence alignment of the *Lymnaea stagnalis* RXR (*Lym*RXR; accession no. AY846875), *Biomphalaria glabrata* RXR (*Bg*RXR; accession no. AAL86461), *Rattus norvegicus* RXR alpha (*Rat*RXRalpha; accession no. NP_036937), and the amphioxus *Branchiostoma floridae* RXR (*Amphi*RXR; accession no. AAM46151) proteins. Note the high conservation of amino acids in the DNA-binding domain (DBD) and the ligand-binding domain (LBD). Amino acid residues reported to interact with the RXR natural ligand *9-cis* RA (Egea et al., 2000) are indicated by green circles above the aligned sequences.

eyes (Fig. 2Diii) or those noticeably reduced in size (Fig. 2Dii). Interestingly, PA024 displayed a higher number of abnormalities than *9-cis* RA, including a number of embryos that exhibited halted development at the trochophore stage (Figs. 2F and J).

Similar experiments were next performed with incubation of embryos in RXR antagonists to determine the effect of inhibiting RXR signaling during embryogenesis. Incubation in the RXR antagonist, HX531 (10^{-6} M), produced shell defects in all embryos (48 of 48 embryos; 100%) but not in eye development (0 of 48 embryos; 0%). Interestingly, incubation in the RXR antagonist, PA452 (10^{-6} M), did not produce any observable defects in either eye or shell development (0 of 44 embryos; 0%; data not shown).

Together, these data strongly suggest a role for RXR in *Lymnaea* development.

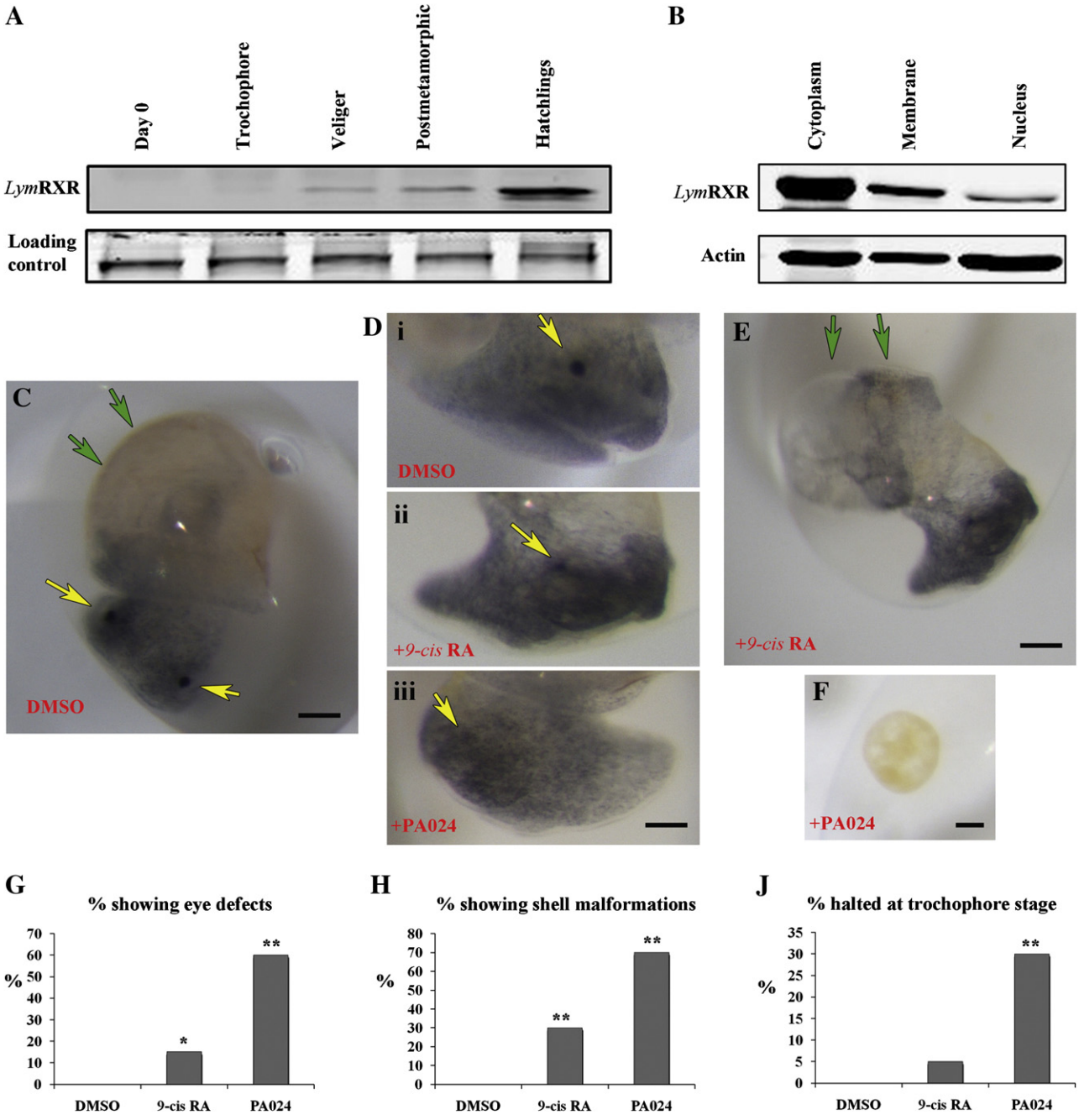

Fig. 2. Embryonic RXR plays a role in *Lymnaea* development. (A) Western blot analysis at five different stages of *Lymnaea* embryogenesis revealed its presence as early as the trochophore stage, and showed maximal expression at hatching. A Coomassie blue stain of the acrylamide gel, before transfer, was used as a loading control. (B) Western blot analysis performed on subcellular fractionations of embryos, using the *Lym*RXR antibody, showed a signal in the cytoplasmic, membrane and nuclear compartments. Actin staining as a control also showed staining in all three compartments. (C) DMSO (0.001%) added to the *Lymnaea* embryos as a vehicle control did not affect development. All of the animals showed normal eye and shell development (compared to embryos in the absence of DMSO). Green arrows indicate the outline of the normally developed shell, and yellow arrows indicate the presence of both eyes. Scale bar: 200 μm. (D) (i) Representative image of a control embryo in DMSO showing the clear presence of an eye (yellow arrow). (ii) Representative example of an underdeveloped eye, reduced in size (yellow arrow), following incubation in the natural RXR ligand, *9-cis* RA (10^{-7} M). (iii) Representative example of an embryo missing an eye (yellow arrow indicates where eye should be located) following incubation in the synthetic RXR agonist PA024 (10^{-7} M). Scale bar (Di–iii): 150 μm. (E) Green arrows indicate malformation of the shell following incubation in *9-cis* RA (10^{-7} M). Scale bar: 200 μm. (F) PA024 halted some embryos at the trochophore stage. Scale bar: 100 μm. For graphs (G) through (J), *9-cis* RA ($n=40$) and PA024 ($n=40$) treatments were compared to the DMSO ($n=40$) treatment ($^{*}P<0.05$, $^{**}P<0.01$).

LymRXR is present in the adult CNS

We have previously shown that both *at*RA and *9-cis* RA exert trophic and tropic effects on adult CNS neurons of *Lymnaea* (Dmetrichuk et al., 2006, 2008), but little is known of the underlying cellular and molecular mechanisms. We next aimed to determine whether RXR expression is maintained following the embryonic stages and, specifically, to determine whether it is present in the adult (nonregenerating) CNS. Western blot analysis of adult *Lymnaea* CNS total protein again revealed a band of approximately 47 kDa in size (Fig. 3A). Using the same *Lym*RXR-specific antibody, we next performed immunohistochemistry on frozen sections of acutely isolated *Lymnaea* CNSs ($n=30$). Immunoreactivity was detected in neurons of all central ganglia. There was strong immunoreactivity in the neuropil and nerve bundles radiating from the brain, suggesting staining of the axonal tracts (Figs. 3B and D). Interestingly, there was little to no apparent staining of RXR (traditionally considered to

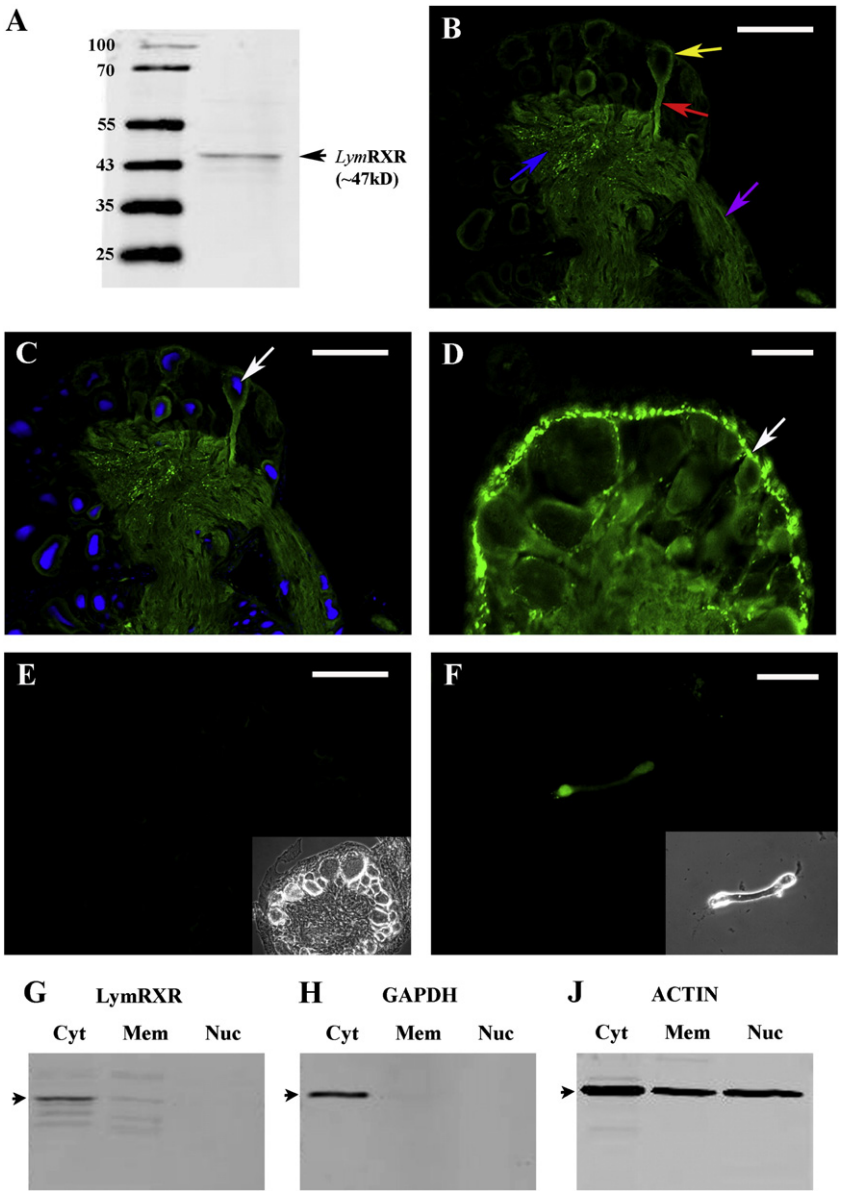

Fig. 3. Cytoplasmic localization of *Lym*RXR in the adult nonregenerating nervous system. (A) Western blot analysis of total protein extracted from the *Lymnaea* CNS showed a band near 47 kDa that closely matches the predicted molecular weight of *Lym*RXR from our cloned sequence. (B and C) *Lym*RXR immunoreactivity was detected in the neurons of ganglia of the CNS (visceral ganglion shown) primarily in the cytoplasm of the cell body (yellow arrow), axons (red arrow), neuropil (blue arrow), and nerve bundles radiating from the brain (purple arrow). Note the absence of RXR staining in the nuclei stained blue using DAPI (C; white arrow). Scale bars: 100 μm. (D) Some ganglia (right pedal ganglion shown) produced strong punctuate-like staining near the periphery (white arrow). Scale bar: 50 μm. (E) Control staining was also performed under the same conditions only in the absence of the primary *Lym*RXR antibody. No immunostaining was visible (inset is a phase-contrast image of the same ganglia). Scale bar: 100 μm. (F) Acutely isolated axons from the *Lymnaea* CNS, plated *in vitro*, also displayed strong immunoreactivity. Inset is a phase-contrast image of the same axon. Scale bar: 30 μm. (G) Western blot performed on subcellular fractionations using the *Lym*RXR antibody showed a signal in the cytoplasmic (Cyt) and membrane (Mem) compartments but not in the nuclear (Nuc) compartment. (H) GAPDH is an abundant glycolytic enzyme in cytoplasm, and a GAPDH antibody, used as a control, showed signal only in the cytoplasmic compartment of the same samples. (J) Actin staining served as a positive control to demonstrate successful isolation of protein from the nuclear compartment.

be a nuclear receptor) in the nuclear region of the neurons, given that there was no RXR signal overlapping with the nuclear DAPI staining (Fig. 3C). Some ganglia also showed strong punctuate-like staining around the periphery of the ganglia (Fig. 3D), which may have been due to RXR immunoreactivity of glial networks and cell bodies in the neural sheath. Control CNS sections with no primary antibody added ($n=6$) demonstrated no immunostaining (Fig. 3E).

To confirm the neuritic localization of RXR, immunofluoresence was also performed on acutely isolated axons. During cell isolation from the intact ganglia, axonal segments up to ~200 μm in length can be acutely isolated, removed from the cell body, and then plated in cell culture (Spencer et al., 2000). We showed that *Lym*RXR immunostaining was indeed present in the acutely isolated axons in culture ($n=3$ of 3; Fig. 3F), which confirmed the above observation that RXR is present in the neuritic processes of neurons in the intact, adult CNS.

To further identify the neuronal compartmentalization of *Lym*RXR in the adult CNSs, we isolated total protein fractions from the cytoplasm, membrane, and nucleus of the adult *Lymnaea* CNS using a Qproteome Cell Compartment kit (Qiagen). In Fig. 3G, Western blot analysis showed a positive signal for RXR in the cytoplasmic and membrane compartments but not in the nucleus. Successful isolation of protein in the nuclear fraction was confirmed by staining for actin, which is now well known to reside in the nucleus (Fig. 3J; Franke, 2004; Bettinger et al., 2004). Anti-GAPDH was also used as a control on the same protein fractions, and as expected, GAPDH showed only positive immunoreactivity in the cytoplasmic compartment (Fig. 3H).

To further confirm the absence of nuclear RXR in the adult CNS cellular fractions, two additional CNS samples were again run, but this time in parallel with embryonic tissue. In the CNS fractions, the RXR was present in both cytoplasmic and membrane compartments but was again absent in the nuclear compartment (data not shown), whereas the embryonic fractions revealed nuclear RXR (as seen in Fig. 2B).

LymRXR is present in the neurites and growth cones of regenerating cultured neurons

Retinoic acid is known to promote neurite regeneration in many species, including neurons from *Lymnaea* (Dmetrichuk et al., 2006, 2008). Our next aim was to determine the localization of RXR immunofluorescence in regenerating central neurons in culture. PeA motor neurons were individually isolated from the intact ganglia and given 24–36 h to regenerate in cell culture (Fig. 4Ai). Following outgrowth, cells were then fixed and stained with the *Lym*RXR antibody. RXR immunoreactivity was visualized in the cell body of every cultured PeA neuron, whether it was actively regenerating neurites or not ($n=96$ of 96). In the neurons that displayed outgrowth ($n=35$), RXR immunoreactivity was observed in the majority of neurites (Fig. 4Aii), although there appeared to be a differential distribution of the RXR signal in the neurites of some cells. Fig. 4Bii illustrates an example of a neurite emanating from a cell body that displayed strong immunoreactivity over most of its length, while another neurite from the same cell body showed very little RXR staining. Furthermore, while most of the growth cones located at the tips of the neurites demonstrated positive immunoreactivity for RXR ($n=95$ of 102), there were some neurites that displayed little, if any, RXR staining along the neurite leading to the growth cone. Immunostaining of the RXR was evident in the central or C-domain of the growth cones, but very little to no staining was evident in the peripheral or P-domain (lamellipodia and filopodia; Fig. 4Cii). Control regenerating PeA neurons, under the same staining conditions except

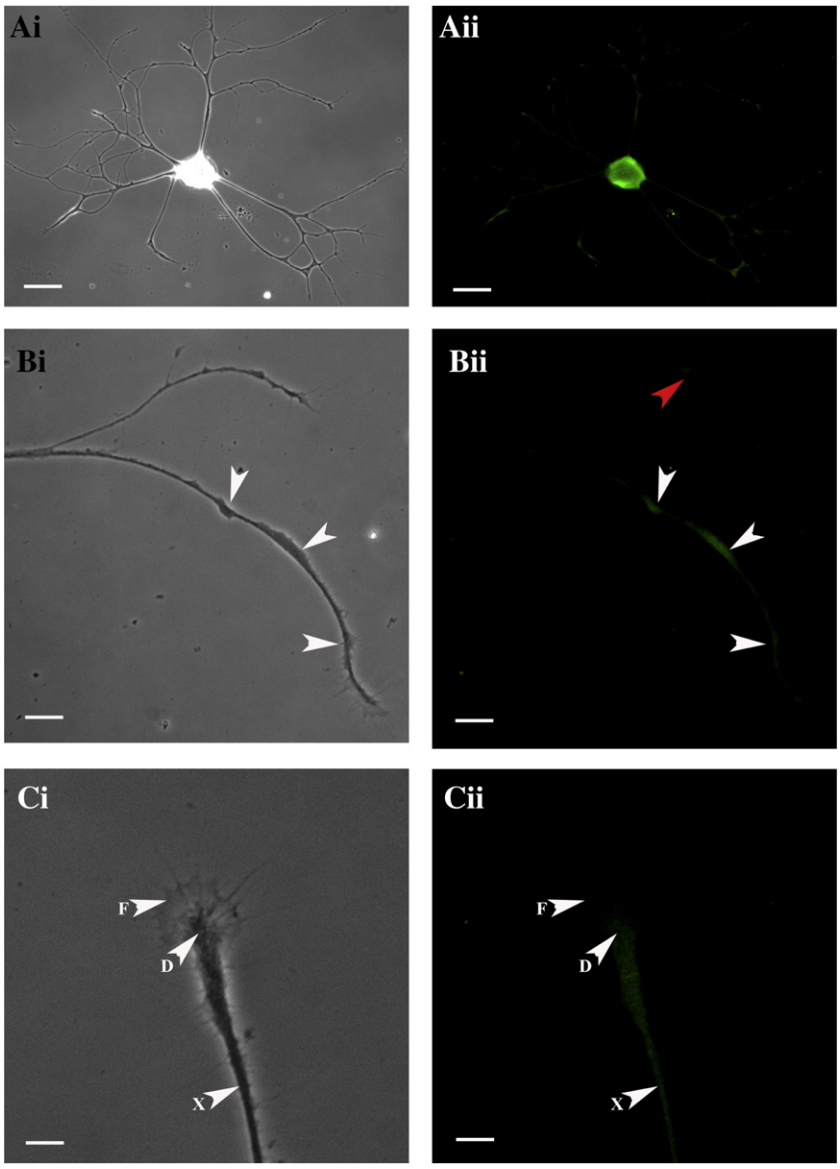

Fig. 4. *Lym*RXR is present in the neurites and growth cones of regenerating motor neurons *in vitro*. (Ai) Phase-contrast image of a cultured *Lymnaea* Pedal A neuron at 48 h in CM with regenerated neurites. (Aii) Immunostaining of the same PeA cell with *Lym*RXR antibody revealed a signal in the cytoplasm of the cell body and the regenerating neurites. Scale bars Ai–ii: 50 μm. (Bi) Phase-contrast image of two neurites from the same cell. (Bii) Immunostaining with the *Lym*RXR antibody showed differential staining in the two branches. White arrows indicate staining of one branch, while the other branch displayed little to no staining (red arrow). Scale bars Bi–ii: 20 μm. (Ci) Phase-contrast image of a PeA growth cone *in vitro*. (Cii) Immunostaining with the *Lym*RXR antibody showed a signal in the neurite leading to the growth cone (X), in the central domain of the growth cone (D), but no staining in the lamellipodia and filopodia (F). Scale bars Ci–ii: 10 μm.

in the absence of primary antibody, did not demonstrate RXR immunoreactivity ($n = 6$; data not shown).

A RXR agonist induced growth cone turning

We have previously shown that retinoic acid (both *all-trans* and *9-cis* isomers) can induce positive growth cone turning of regenerating *Lymnaea* growth cones (Dmetrichuk et al., 2006, 2008; Farrar et al., 2009). We have also shown that this growth cone turning is dependent on protein synthesis and calcium influx (Farrar et al., 2009). Because we had demonstrated that this turning response occurred in isolated growth cones and involved a localized, nongenomic mechanism, we had not previously investigated a role for the retinoid receptor. However, having now determined that the RXR is present in the regenerating growth cones and neurites, we next investigated whether it was involved in the localized growth cone turning response to RA.

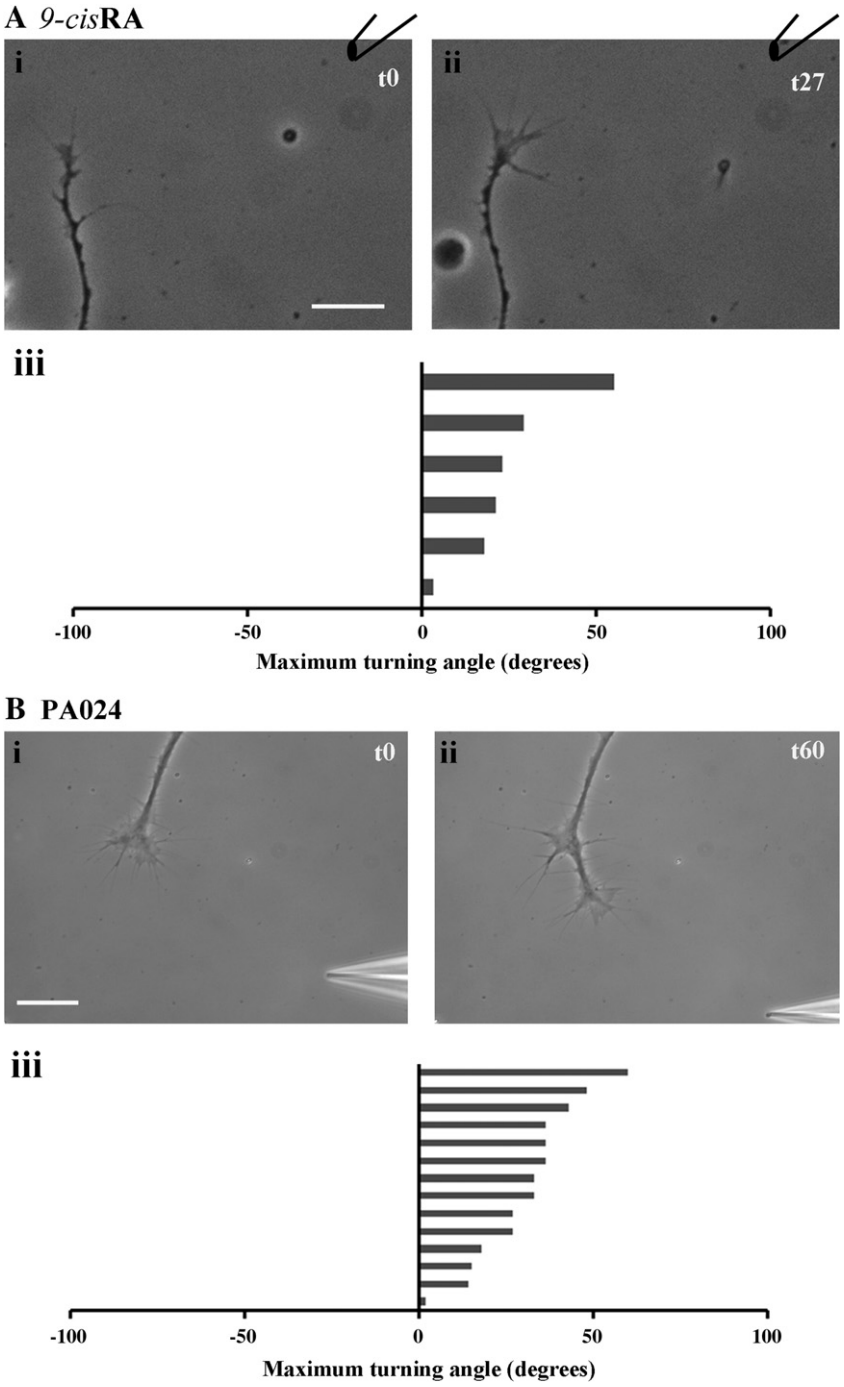

Fig. 5. Intact PeA growth cones turn toward the RXR agonist. (A) (i–ii) Representative example of a PeA growth cone turning toward *9-cis* RA (i: 0 min; ii: 27 min after start of application). Approximate pipette location is indicated. Scale bar: 30 μm. (iii) Histogram depicts maximum turning angle of intact growth cones to *9-cis* RA, and each bar represents one growth cone. Positive values represent a turn toward the pipette and negative values represent a turn away from the pipette. (B) (i–ii) Representative example of a PeA growth cone turning toward the RXR pan-agonist PA024 (i: 0 min, ii: 60 min after start of application). Scale bar: 30 μm. (iii) Histogram depicts maximum turning angle of intact growth cones to PA024, and each bar represents one growth cone. Positive values represent a turn toward the pipette and negative values represent a turn away from the pipette. (C) (i–ii) Representative example of a PeA growth cone that did not turn toward DMSO (vehicle control) (i: 0 min, ii: 26 min after start of application). Scale bar: 30 μm. (iii) Histogram depicts maximum turning angle of intact growth cones to DMSO, and each bar represents one growth cone. Positive values represent a turn toward the pipette and negative values represent a turn away from the pipette.

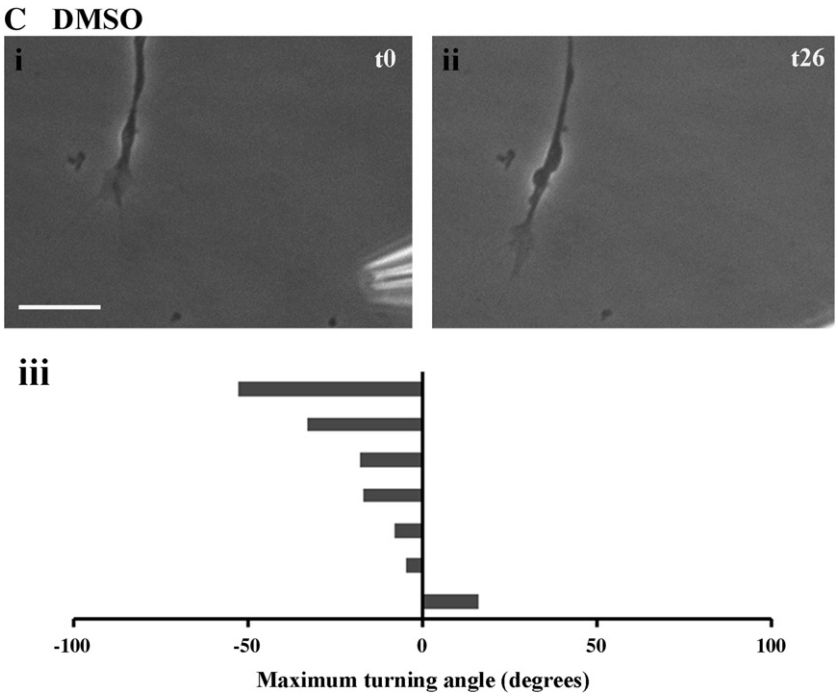

Fig. 5 (*continued*).

We have previously reported growth cone turning toward *9-cis* RA in VF neurons (Dmetrichuk et al., 2008). However, *9-cis* RA was applied again in this study to directly compare its effects on PeA growth cone behaviour with those of a RXR agonist. Here, we showed that *9-cis* RA produced attractive growth cone turning of intact PeA neurites with an average turning angle of 24.8°±7° ($n=6$; Fig. 5Ai–iii). We next pressure-applied the RXR pan-agonist PA024 onto the PeA growth cones to determine whether it would mimic the growth cone turning induced by *9-cis* RA. Indeed, PA024 induced positive growth cone turning of intact neurites with a mean angle of 30.6°±4.0° ($n=14$; Fig. 5Bi–iii). As PA024 is dissolved in DMSO, control experiments with DMSO in the pipette were also performed and were shown not to produce positive growth cone turning (−16.9°±8.3°; $n=7$; Fig. 5Ci–iii). Statistical analysis revealed that growth cone turning toward the RXR agonist PA024 was significantly different from the DMSO control ($P<0.05$) but was not significantly different from growth cone turning toward *9-cis* RA.

We previously showed that neurites physically transected and isolated from their cell body could also turn toward RA, demonstrating that a local mechanism was involved. We next aimed to determine whether the RXR agonist would also induce turning in growth cones of transected neurites, physically isolated from their cell body. Once again, PA024 induced attractive growth cone turning (Fig. 6Ai–iv) with a mean angle of 23.9°±13.8° ($n=11$; Fig. 6B), which was not significantly different from that produced by PA024 in intact neurites. All intact and isolated neurite data are summarized in Fig. 6C.

The RXR agonist-induced growth cone turning is inhibited in the presence of an RXR antagonist

We next aimed to determine whether we could block the RXR agonist-induced growth cone turning in the presence of a RXR antagonist. First of all, we showed that application of the RXR agonist PA024 (10^{-6} M) to intact PeA growth cones in the presence of the vehicle control (DMSO; 0.01%) produced growth cone turning (Fig. 7Ai–ii) with a mean angle of 36.3°±8.7° ($n=7$; Fig. 7B). We next applied the RXR agonist PA024 (10^{-6} M) in the presence of the RXR antagonist PA452 (final bath concentration of 10^{-6} M). In the presence of the RXR antagonist PA452, the mean turning angle in response to application of the agonist was significantly reduced to 3.3°±10.3° ($n=9$; $P<0.05$; Fig. 7E). However, despite the overall reduced mean turning angle, six of the nine growth cones maintained a positive turn toward the RXR agonist in the presence of PA452 (Fig. 7Ci–ii), with an average turning angle of 22.5°±4.0°. The remaining three growth cones turned away from the pipette (Fig. 7Di–ii), with a mean turning angle of −35°±12.3° ($n=3$).

We next chose to use a different RXR antagonist, HX531, to determine whether we could block the agonist-induced growth cone turning. In these experiments, we recorded the growth cone turning angle in response to application of the RXR agonist in the presence of HX531 (10^{-6} M). This time, the growth cone turning toward PA024 was completely abolished in 9 of the 10 growth cones tested (Fig. 7Fi–ii) The mean turning angle in the presence of HX531 was −19.4°±7.5° away from the pipette (Fig. 7G), which was significantly different from the turning angle in DMSO ($P<0.01$; Fig. 7H). We also confirmed that the turning of isolated PeA growth cones toward the RXR agonist was abolished in the presence of HX531 ($n=4$ of 4; data not shown).

In summary, these data suggest that RXR, located in neurites and growth cones of regenerating neurons, plays a novel, nongenomic role in RA-induced growth cone turning, at least in *Lymnaea* PeA motor neurons.

Discussion

In this study, we have cloned a full-length RXR from the mollusc, *L. stagnalis* and have shown that this retinoid receptor is present in the developing embryo, as well as in the nonregenerating, adult CNS, where it was found in the neuritic domains of central neurons. Using regenerating cultured motor neurons, we have provided evidence that it plays a role in the chemotropic response of growth cones to retinoic acid.

RXRs are highly conserved members of the steroid/retinoid family of nuclear hormone receptors and have been identified in species ranging from the phylogenetically oldest metazoan phylum (the sponge) to mammals (Mangelsdorf et al., 1992). Interestingly, the

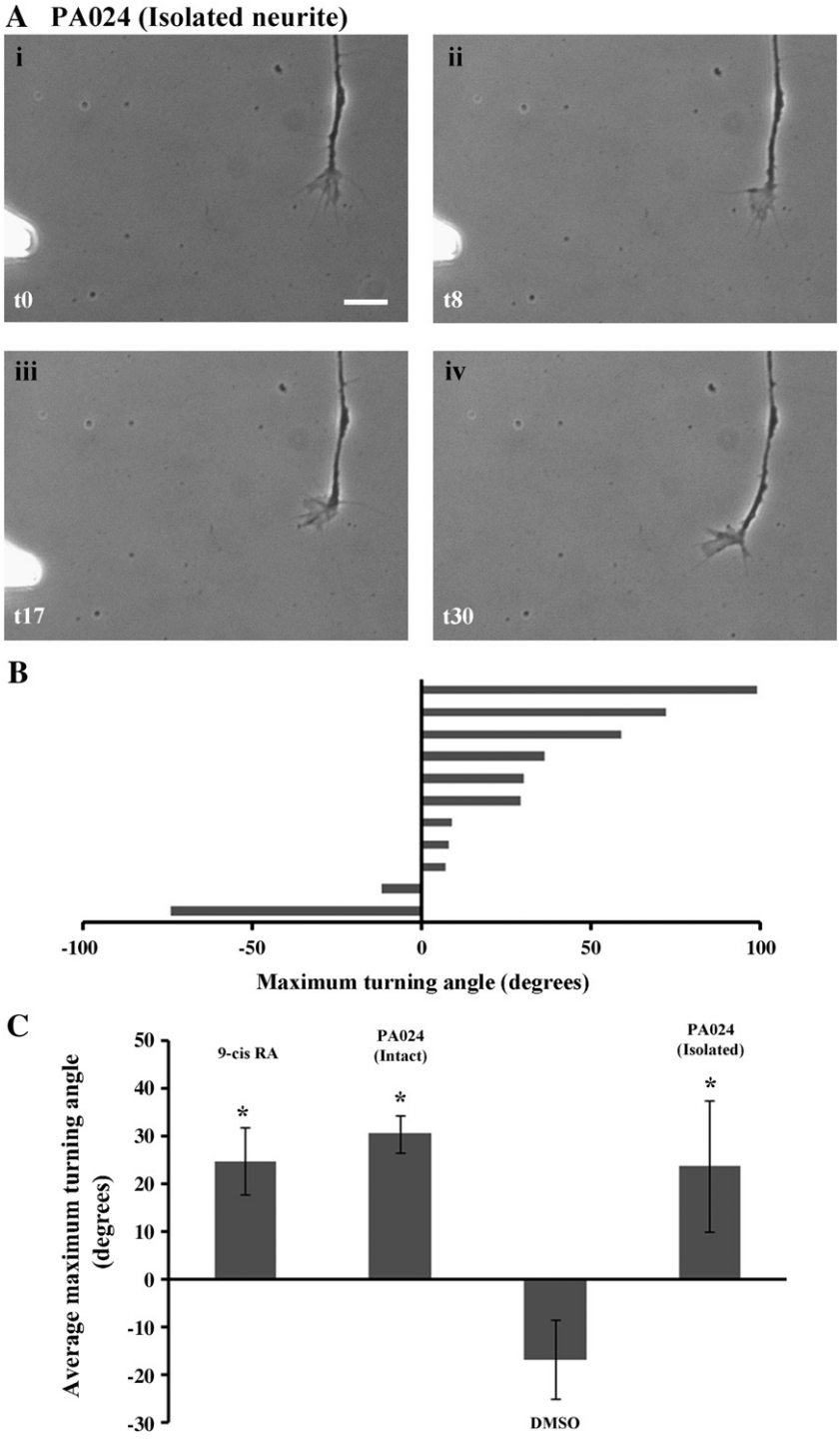

Fig. 6. Isolated PeA growth cones turn toward the RXR agonist. Neurites were physically isolated from the cell bodies and the RXR agonist PA024 was applied to the isolated growth cones. (A) Representative example of an isolated growth cone turning toward PA024 (i) before PA024 application and following (ii) 8 min, (iii) 17 min, and (iv) 30 min of PA024 application. Scale bar: 25 μm. (B) Histogram depicts maximum turning angle of isolated growth cones to PA024, and each bar represents one growth cone. Positive values represent a turn toward the pipette and negative values represent a turn away from the pipette. (C) Summary graph of mean growth cone turning angles under all conditions. Error bars represent standard error of the mean (SEM). $^{*}P<0.05$ when compared to DMSO controls.

RXR from *Lymnaea* (a lophotrochozoan, nonchordate mollusc and true invertebrate outside of the chordate lineage) shows higher amino acid identity with the rat RXRα than the RXR from *Polyandrocarpa*, a urochordate species and closest living relative of the vertebrates (Borel et al., 2009). Furthermore, it has previously been shown that a molluscan RXR (from *B. glabrata*; *Bg*RXR) functionally interacts with vertebrate RXR-binding partners, strongly suggesting that retinoid signalling may be shared between the lophotrochozoan branch of the protostomes and the deuterostomes (which contain the chordate branch).

RXRs from mammals have been studied most extensively, and it has been shown that they can form homodimers, heterodimers, or even homotetramers and regulate target gene expression when bound with their proposed ligand, *9-cis* RA (Kersten et al., 1995). Interestingly, the amino acids in mouse RXRα that interacted with 9-*cis* RA (Egea et al., 2000) are all perfectly conserved in the *Bg*RXR

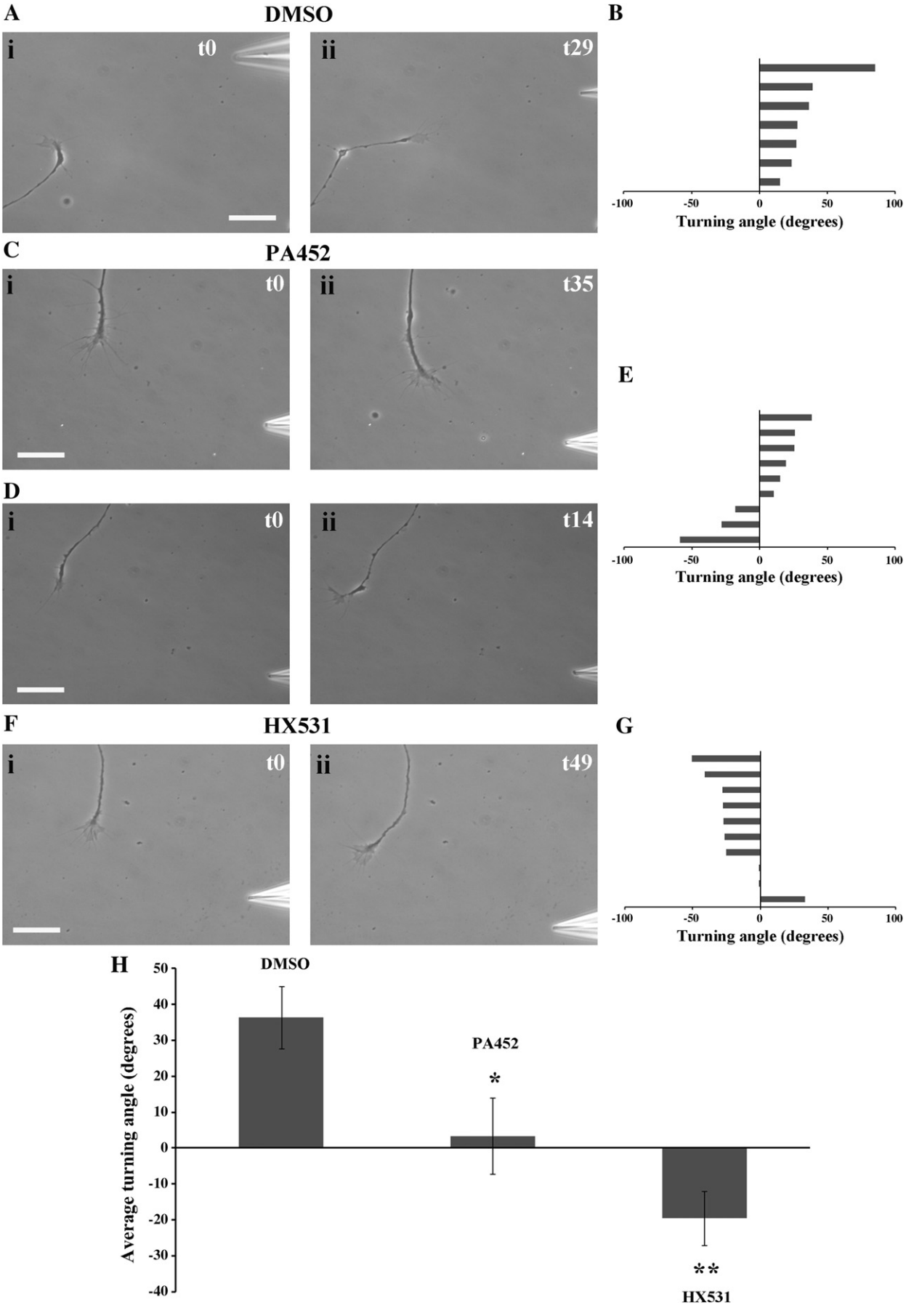
A
DMSO
i
t0
ii
t29
B
-100
-50
0
50
100
Turning angle (degrees)
C
PA452
i
t0
ii
t35
E
-100
-50
0
50
100
Turning angle (degrees)
D
i
t0
ii
t14
F
HX531
i
t0
ii
t49
G
-100
-50
0
50
100
Turning angle (degrees)
H
DMSO
PA452
*
**
HX531
Average turning angle (degrees)
50
40
30
20
10
0
-10
-20
-30
-40

sequence (Bouton et al., 2005) as well as in our *Lym*RXR sequence. The *Bg*RXR can also transactivate transcription when treated with exogenous *9-cis* RA (Bouton et al., 2005). Although there is evidence that invertebrate RXRs, like the vertebrate RXRs, bind *9-cis* RA (Kostrouch et al., 1998), a recent study showed that both *9-cis* and *all-trans* RA isomers bind with similar affinities to the locust RXR (Nowickyj et al., 2008). *All-trans* RA also upregulates RXR mRNA in the marine sponge *Suberites domuncula* (Wiens et al., 2003) and increases the abundance of RXR mRNA in blastemas during limb regeneration in the fiddler crab *Uca pugilator* (Chung et al., 1998). We have recently shown using HPLC and MS that both *9-cis* and *all-trans* RA isomers are present in the *Lymnaea* CNS (Dmetrichuk et al., 2008), and so we cannot rule out that both isomers may be natural ligands for *Lym*RXR.

RXR expression in the developing embryo

Our results indicate that RXR expression occurred in *Lymnaea* embryos as early as the trochophore stage and continued through the postmetamorphic stage, reaching maximal expression at hatching (juvenile form). We do not know whether this expression occurred in the nervous system or whether it was associated with other organs. However, demonstration of RXR expression at the veliger stage correlates with the first ultrastructural detection of cerebral and pedal ganglia (Nagy and Elekes, 2000). However, at this developmental stage, the authors detected only two to three cells per ganglia, and only a small number of axon profiles, with no evidence of filopodial processes or developing synapses. In the later stages of embryonic development (postmetamorphic, adult-like stage), when we observed increased RXR expression, Nagy and Elekes (2000) observed the whole central ring ganglia and neuropil densely packed with axon profiles, although there was no evidence of glia or the neural sheath. Interestingly, the authors proposed that the absence of the neural sheath during these stages would facilitate trophic and/or hormonal influences in the developing ganglia, which we propose may include trophic or tropic support provided by RA. By hatching, at which stage we saw maximal RXR expression, Nagy and Elekes (2000) demonstrated that the CNS had significantly increased in size, with enlarged neuropil and more axon profiles, as well as the first evidence of glia and a neuronal sheath. In summary, we found that RXR is expressed in our *Lymnaea* embryos before the metamorphic stage, which is thought to be the time when the neuropil is undergoing substantial reorganization, likely indicating a period of substantial migration and reorganization of axons (Nagy and Elekes, 2000). It is quite feasible, therefore, that the RXR plays a role in *Lymnaea* nervous system development.

Creton et al. (1993) have previously demonstrated that application of 10^{-7} M RA during the gastrulation stage of *Lymnaea* embryos produced only eye defects (no shell or CNS deformations) and only in 15% of embryos. In our study, both eye and shell deformations were found following incubation in 10^{-7} M *9-cis* RA and PA024. Although not explicitly stated, we presume that the isomer used in the previous studies was *at*RA, possibly explaining the difference in teratogenicity observed. If this is indeed the case, it might suggest that *9-cis* RA is a more potent teratogen in *Lymnaea* than *at*RA. It should be noted, however, that in vertebrates, *9-cis* RA activates RARs, in addition to RXRs. It is thus possible that *9-cis* RA will also be activating a RAR. We believe this unlikely, as despite our recent cloning of an RAR in *Lymnaea*, we have not yet been able to detect the protein in the early embryonic stages of development (Carter and Spencer, 2009). This suggests that if the RAR is indeed present, it is likely at much lower levels than the RXR. In support of our hypothesis that *9-cis* RA is likely acting via the RXR, the effects of *9-cis* RA were closely mimicked by PA024, which was developed as a RXR-selective agonist (Ohta et al., 2000). The demonstration that the RXR was present in the nuclear compartments of embryonic protein fractions strongly suggests that the teratogenic effects of the RXR agonist and *9-cis* RA were likely mediated via genomic actions of the RXR. However, we were unable to distinguish cellular localization of the RXR in specific tissues of the embryo, and as its presence was also shown in cytoplasmic and membrane compartments, we cannot rule out the possibility of nongenomic effects during embryogenesis.

Cytoplasmic localization of RXR and its role in growth cone turning behaviour

Although we could not determine where in the *Lymnaea* embryo the RXR was specifically expressed, we were able to clearly determine the expression and subcellular localization of RXR in neurons of the adult CNS. We found that *Lym*RXR protein was localized to the cytoplasm and membrane of adult neurons, and staining in the neuropil strongly suggested localization in the axonal tracts. This axonal staining was further confirmed following immunostaining of acutely isolated axonal segments from the CNS, plated in culture. These findings were interesting because RXR traditionally acts as a ligand-activated transcription factor and would thus be expected to show nuclear localization. Some nuclear receptors including steroid and thyroid hormone receptors can, however, shuttle between the nucleus and the cytoplasm (DeFranco, 1997; Kaffman and O'Shea, 1999). RXRα also shuttles between the nucleus and cytoplasm (either in the absence or presence of its ligand *9-cis* RA) and can also act as a shuttle for the orphan receptor TR3, a process stimulated by *9-cis* RA (Lin et al., 2004). *9-cis* RA was also found to enhance nuclear translocation of RXRα in COS-7 cells by associating with importinβ bound to a RXRα nuclear localization signal (NLS). Phosphorylation of a conserved serine/threonine in the NLS of nuclear receptors inhibits their ability to translocate to the nucleus, and if threonine is mutated into aspartic acid in human RXRα, nuclear localization is significantly hindered (Sun et al., 2007). Our *Lym*RXR protein shares an identical NLS with the human RXRα, suggesting that phosphorylation of this threonine in *Lym*RXR may play a role in its cytoplasmic localization.

In embryonic cultured rat hippocampal neurons, RXR isoforms exhibited differential nuclear and cytoplasmic staining. All RXR isoforms except RXRβ2 were shown to be present in the cytoplasm, but RXRα was the only RXR isoform that was expressed in the axonal compartment (Calderon and Kim, 2007). RXRα was also evident in the axonal compartment of newly regenerating axons following sciatic nerve crush injury (Zhelyaznik and Mey, 2006), possibly supporting a role for RXR in neural regeneration. In our regenerating adult *Lymnaea* neurons, RXR immunoreactivity was found in most of

Fig. 7. The agonist-induced growth cone turning is inhibited by RXR antagonists. The RXR agonist, PA042, was pressure-applied (10^{-6} M) to intact PeA growth cones in the presence of either DMSO (vehicle) or RXR antagonists in the bath. (A) An example of a growth cone that turned toward the RXR agonist PA024 in the presence of bath-applied DMSO (0.01%). (i) Before application of PA024 and (ii) following 29 min of application. Note that the growth cone continued to grow in the direction of the pipette. Scale bar: 30 μm. (B) Histogram depicts turning angles of intact growth cones to PA024 in the presence of DMSO, and each bar represents one growth cone. (C) Representative example of a growth cone that turned toward PA024 in the presence of bath-applied RXR antagonist, PA452 (10^{-6} M). (i) Before application of PA024 and (ii) following 35 min of application. Scale bar: 30 μm. (D) Representative example of a growth cone that turned away from PA024 in the presence of bath-applied RXR antagonist, PA452 (10^{-6} M). (i) Before application of PA024 and (ii) following 14 min of application. Scale bar: 30 μm. (E) Histogram depicts turning angles of intact growth cones in response to PA024 in the presence of the RXR antagonist PA452. (F) Representative example of a growth cone that turned away from PA024 in the presence of bath-applied RXR antagonist, HX531 (10^{-6} M). (i) Before application of PA042 and (ii) following 49 min of application. Scale bar: 30 μm. (G) Histogram depicts turning angles of intact growth cones to PA024 in the presence of the RXR antagonist HX531. (H) Summary graph of mean growth cone turning angles in response to PA042 in the presence of either DMSO or RXR antagonists. Error bars represent standard error of the mean (SEM). $^{*}P<0.05$ and $^{**}P<0.01$, when compared to DMSO controls.

the neuritic processes, although some differential distribution between neurites of the same cell was observed. The cellular distribution of RXRα has been shown to be time-dependent after contusion injury of rat spinal cord, varying between dendritic and nuclear localization, depending on days following surgery (Schrage et al., 2006). Interestingly, these authors also determined the presence of retinoid receptors in the cytoplasm of neurons and glia cells in the *noninjured* spinal cord similar to our observations of *Lym*RXR distribution in the nonregenerating CNSs.

Having demonstrated neuritic localization of *Lym*RXR, both in nonregenerating and regenerating neurons, we next demonstrated that a RXR pan-agonist, applied to the growth cones of cultured PeA motor neurons, induced growth cone turning and mimicked the growth cone response to *9-cis* RA (and *all-trans* RA seen previously; Dmetrichuk et al., 2008). We should note, however, that this RXR pan-agonist was designed for the vertebrate RXR, and we have no knowledge of its binding affinity to the *Lym*RXR (although our *Lym*RXR shows >80% homology to the LBD of vertebrate RXRα and the *9-cis* RA-interacting amino acids are 100% conserved). Likewise, both RXR antagonists used in this study were designed against the vertebrate RXR, yet our data show that both antagonists significantly reduced the growth cone turning response to the RXR agonist. Interestingly, the results with the RXR antagonist PA452 were more ambiguous than with the antagonist HX531. In the presence of PA452, although the overall mean turning angle was significantly reduced compared to controls, the RXR agonist was still able to induce a positive turning response in six of the nine growth cones tested. This was not the case with HX531, where only 1 of 10 growth cones showed any positive turning response to the RXR agonist. In 9 of the 10 growth cones, the attractive turning was completely abolished in HX531. It appears, therefore, that HX531 is a more effective antagonist for the *Lym*RXR than PA452, although the reason for this is not known. This is also supported by our finding that HX531 produced some teratogenic effects during *Lymnaea* embryogenesis, whereas PA452 had no obvious effect.

Together with our evidence that *Lym*RXR is localized in neurites and growth cones, our data showing RXR agonist-induced growth cone turning (that is subsequently inhibited in the presence of a RXR antagonist) strongly implicate a role for RXR in regeneration and growth cone guidance. In support of this conclusion, Zhelyaznik and Mey (2006) recently showed that RXRα transcript and protein levels were upregulated after sciatic nerve crush injury in rats. Furthermore, they demonstrated that the increase in RXRα immunoreactivity after injury did not occur in the degenerating nerve stump but was observed in regenerating axons. This led the authors to propose that regulation of RXRα was connected with processes related to axon growth.

As mentioned previously, a RAR has also recently been cloned from the *Lymnaea* CNS (Carter and Spencer, 2009). We do not yet know whether this receptor also exists outside the nucleus and thus cannot rule out the possibility that the RXR may be acting in conjunction with the RAR to produce growth cone turning. We also have not yet determined whether the endogenous retinoid isomers might be activating other parallel pathways (such as direct interactions with enzymes) to produce growth cone turning, and so the exact contribution of RXR activation in the turning response produced by 9-*cis* and *at*RA is yet to be determined.

A nongenomic role for RXR in growth cone turning

A significant finding of our current study is that the RXR agonist also produced growth cone turning of isolated growth cones, in the absence of the cell body and nucleus, suggesting a novel, nongenomic role in growth cone steering. There are a number of reports in the literature of RA exerting nongenomic actions. Some of these involve activation of messengers such as ERK1/2 and RSK (Aggarwal et al., 2006) and direct binding with PKC (Ochoa et al., 2003). Other reports implicate nongenomic actions of RARs. For example, RA rapidly enhanced spontaneous acetylcholine release at developing neuromuscular synapses in *Xenopus* cell culture and an RARβ agonist alone mimicked this effect (Liao et al., 2004). Another study demonstrated RARα in rat hippocampal dendrites and demonstrated a nongenomic role in the translational control of GluR1 (Poon and Chen, 2008). The activation of phosphatidylinositol-3-kinase during RA-induced differentiation of neuroblastoma cells is also proposed to occur via nongenomic actions of the RAR (Masia et al., 2007). Although there are no previous reports of nongenomic actions of RXR in the CNS, RXRs were recently shown to exert nongenomic effects in human platelets (Moraes et al., 2007). RXRα and RXRβ were present in the cytosolic and membrane fractions of the platelets, and (despite the lack of a nucleus) the proposed RXR ligand, *9-cis* RA, inhibited platelet aggregation. It was determined that the platelet RXR bound to the G protein $Gq_{/11}$ and that this association was strengthened within 3 min of *9-cis* RA stimulation. This led the authors to propose that the RXR–$Gq_{/11}$ binding event induced by *9-cis* RA prevents $Gq_{/11}$ from activating Rac and the subsequent aggregation-dependant pathways (Moraes et al., 2007). Although we have previously shown a role for protein synthesis and calcium influx in the nongenomic actions of RA in *Lymnaea* growth cone turning, where and how the RXR may be involved in this signaling pathway are currently unknown.

In summary, we have cloned the first retinoid receptor in the mollusc *L. stagnalis* and demonstrated its presence and potential role during embryonic development. Significantly, we have demonstrated a cytoplasmic and neuritic localization for *Lym*RXR, both in non-regenerating adult CNSs and in regenerating motor neurons *in vitro*. Finally, we have shown that *Lym*RXR is present in regenerating growth cones and provide the first evidence that RXR may play a novel, nongenomic role in mediating the chemotropic effects of RA.

Acknowledgments

This work was supported by Discovery Grants to G.E.S. and R.L.C. from the Natural Sciences and Engineering Research Council (NSERC) of Canada. C.J.C. and N.R.F. were supported by scholarships from NSERC (Canada). We are very grateful to Dr. Hiroyuki Kagechika (University of Tokyo, Japan) for the kind gift of the RXR agonist, PA024, as well as the RXR antagonists, PA452 and HX531. We would also like to thank Dr. Zhong-Ping Feng (University of Toronto, Canada) for her assistance in reading the manuscript.

References

Aggarwal, S., Kim, S.W., Cheon, K., Tabassam, F.H., Yoon, J.H., Koo, J.S., 2006. Nonclassical action of retinoic acid on the activation of the cAMP response element-binding protein in normal human bronchial epithelial cells. Mol. Biol. Cell 17, 566–575.

Albalat, R., Canestro, C., 2009. Identification of Aldh1a, Cyp26 and RAR orthologs in protostomes pushes back the retinoic acid genetic machinery in evolutionary time to the bilaterian ancestor. Chem. Biol. Interact. 178, 188–196.

Bettinger, B.T., Gilbert, D.M., Amberg, D.C., 2004. Actin up in the nucleus. Nat. Rev. Mol. Cell Biol. 5, 410–415.

Biesalski, H.K., Doepner, G., Tzimas, G., Gamulin, V., Schroder, H.C., Batel, R., Nau, H., Muller, W.E., 1992. Modulation of *myb* gene expression in sponges by retinoic acid. Oncogene 7, 1765–1774.

Borel, F., de Groot, A., Juillan-Binard, C., de Rosny, E., Laudet, V., Pebay-Peyroula, E., Fontecilla-Camps, J.C., Ferrer, J.L., 2009. Crystal structure of the ligand-binding domain of the retinoid X receptor from the ascidian *Polyandrocarpa misakiensis*. Proteins 74, 538–542.

Bouton, D., Escriva, H., de Mendonca, R.L., Glineur, C., Bertin, B., Noel, C., Robinson-Rechavi, M., de Groot, A., Cornette, J., Laudet, V., Pierce, R.J., 2005. A conserved retinoid X receptor (RXR) from the mollusk *Biomphalaria glabrata* transactivates transcription in the presence of retinoids. J. Mol. Endocrinol. 34, 567–582.

Calderon, F., Kim, H.Y., 2007. Role of RXR in neurite outgrowth induced by docosahexaenoic acid. Prostaglandins Leukot. Essent. Fatty Acids 77, 227–232.

Carter, C.J. and Spencer, G.E., 2009. Cloning of a retinoic acid receptor (RAR) from the CNS of a non-chordate, invertebrate protostome and its role in embryonic development. Program# 225.11, 2009 Neuroscience Meeting Planner. Washington, DC: Society for Neuroscience. Online.

Chung, A.C., Durica, D.S., Clifton, S.W., Roe, B.A., Hopkins, P.M., 1998. Cloning of crustacean ecdysteroid receptor and retinoid-X receptor gene homologs and elevation of retinod-X receptor mRNA by retinoic acid. Mol. Cell. Endocrinol. 139, 209–227.

Corcoran, J., Shroot, B., Pizzey, J., Maden, M., 2000. The role of retinoic acid receptors in neurite outgrowth from different populations of embryonic mouse dorsal root ganglia. J. Cell Sci. 113 (Pt 14), 2567–2574.

Creton, R., Zwaan, G., Dohmen, R., 1993. Specific developmental defects in molluscs after treatment with retinoic acid during gastrulation. Dev. Growth Differ. 35, 357–364.

DeFranco, D.B., 1997. Subnuclear trafficking of steroid receptors. Biochem. Soc. Trans. 25, 592–597.

Dmetrichuk, J.M., Spencer, G.E., Carlone, R.L., 2005. Retinoic acid-dependent attraction of adult spinal cord axons towards regenerating newt limb blastemas *in vitro*. Dev. Biol. 281, 112–120.

Dmetrichuk, J.M., Carlone, R.L., Spencer, G.E., 2006. Retinoic acid induces neurite outgrowth and growth cone turning in invertebrate neurons. Dev. Biol. 294, 39–49.

Dmetrichuk, J.M., Carlone, R.L., Jones, T.R., Vesprini, N.D., Spencer, G.E., 2008. Detection of endogenous retinoids in the molluscan CNS and characterization of the trophic and tropic actions of 9-*cis* retinoic acid on isolated neurons. J. Neurosci. 28, 13014–13024.

Durston, A.J., Timmermans, J.P., Hage, W.J., Hendriks, H.F., de Vries, N.J., Heideveld, M., Nieuwkoop, P.D., 1989. Retinoic acid causes an anteroposterior transformation in the developing central nervous system. Nature 340, 140–144.

Egea, P.F., Mitschler, A., Rochel, N., Ruff, M., Chambon, P., Moras, D., 2000. Crystal structure of the human RXRalpha ligand-binding domain bound to its natural ligand: 9-*cis* retinoic acid. EMBO J. 19, 2592–2601.

Farrar, N.R., Dmetrichuk, J.M., Carlone, R.L., Spencer, G.E., 2009. A novel, nongenomic mechanism underlies retinoic acid-induced growth cone turning. J. Neurosci. 29, 14136–14142.

Franke, W.W., 2004. Actin's many actions start at the genes. Nat. Cell Biol. 6, 1013–1014.

Gu, P.L., Gunawardene, Y.I., Chow, B.C., He, J.G., Chan, S.M., 2002. Characterization of a novel cellular retinoic acid/retinol binding protein from shrimp: expression of the recombinant protein for immunohistochemical detection and binding assay. Gene 288, 77–84.

Gudas, L.J., 1994. Retinoids and vertebrate development. J. Biol. Chem. 269, 15399–15402.

Heyman, R.A., Mangelsdorf, D.J., Dyck, J.A., Stein, R.B., Eichele, G., Evans, R.M., Thaller, C., 1992. 9-*cis* Retinoic acid is a high affinity ligand for the retinoid X receptor. Cell 68, 397–406.

Kaffman, A., O'Shea, E.K., 1999. Regulation of nuclear localization: a key to a door. Annu. Rev. Cell Dev. Biol. 15, 291–339.

Kersten, S., Kelleher, D., Chambon, P., Gronemeyer, H., Noy, N., 1995. Retinoid X receptor alpha forms tetramers in solution. Proc. Natl. Acad. Sci. U. S. A. 92, 8645–8649.

Knutson, D.C., Clagett-Dame, M., 2008. *at*RA Regulation of *NEDD9*, a gene involved in neurite outgrowth and cell adhesion. Arch. Biochem. Biophys. 477, 163–174.

Kostrouch, Z., Kostrouchova, M., Love, W., Jannini, E., Piatigorsky, J., Rall, J.E., 1998. Retinoic acid X receptor in the diploblast, *Tripedalia cystophora*. Proc. Natl. Acad. Sci. U. S. A. 95, 13442–13447.

Liao, Y.P., Ho, S.Y., Liou, J.C., 2004. Non-genomic regulation of transmitter release by retinoic acid at developing motoneurons in *Xenopus* cell culture. J. Cell Sci. 117, 2917–2924.

Lin, X.F., Zhao, B.X., Chen, H.Z., Ye, X.F., Yang, C.Y., Zhou, H.Y., Zhang, M.Q., Lin, S.C., Wu, Q., 2004. RXRalpha acts as a carrier for TR3 nuclear export in a 9-*cis* retinoic acid-dependent manner in gastric cancer cells. J. Cell Sci. 117, 5609–5621.

Lohof, A.M., Quillan, M., Dan, Y., Poo, M.M., 1992. Asymmetric modulation of cytosolic cAMP activity induces growth cone turning. J. Neurosci. 12, 1253–1261.

Maden, M., 2007. Retinoic acid in the development, regeneration and maintenance of the nervous system. Nat. Rev. Neurosci. 8, 755–765.

Maden, M., Hind, M., 2003. Retinoic acid, a regeneration-inducing molecule. Dev. Dyn. 226, 237–244.

Maden, M., Keen, G., Jones, G.E., 1998. Retinoic acid as a chemotactic molecule in neuronal development. Int. J. Dev. Neurosci. 16, 317–322.

Mangelsdorf, D.J., Borgmeyer, U., Heyman, R.A., Zhou, J.Y., Ong, E.S., Oro, A.E., Kakizuka, A., Evans, R.M., 1992. Characterization of three RXR genes that mediate the action of 9-*cis* retinoic acid. Genes Dev. 6, 329–344.

Mansfield, S.G., Cammer, S., Alexander, S.C., Muehleisen, D.P., Gray, R.S., Tropsha, A., Bollenbacher, W.E., 1998. Molecular cloning and characterization of an invertebrate cellular retinoic acid binding protein. Proc. Natl. Acad. Sci. U. S. A. 95, 6825–6830.

Masia, S., Alvarez, S., de Lera, A.R., Barettino, D., 2007. Rapid, nongenomic actions of retinoic acid on phospatidylinositol-3-kinase signaling pathway by the retinoic acid receptor. Mol. Endocrinol. 21, 2391–2402.

Meshcheryakov, V.N., 1972. The common pond snail *Lymnaea stagnalis*. In: Dettlaff, T.A., Vassetzky, S.G. (Eds.), Animal Species for the Developmental Studies. Consultants Bureau, New York, pp. 69–132.

Mey, J., McCaffery, P., 2004. Retinoic acid signaling in the nervous system of adult vertebrates. Neuroscientist 10, 409–421.

Moraes, L.A., Swales, K.E., Wray, J.A., Damazo, A., Gibbins, J.M., Warner, T.D., Bishop-Bailey, D., 2007. Nongenomic signaling of the retinoid X receptor through binding and inhibiting Gq in human platelets. Blood 109, 3741–3744.

Muley, P.D., McNeill, E.M., Marzinke, M.A., Knobel, K.M., Barr, M.M., Clagett-Dame, M., 2008. The *at*RA-responsive gene neuron navigator 2 functions in neurite outgrowth and axonal elongation. Dev. Neurobiol. 68, 1441–1453.

Nagy, T., Elekes, K., 2000. Embryogenesis of the central nervous system of the pond snail *Lymnaea stagnalis* L. An ultrastructural study. J. Neurocytol. 29, 43–60.

Nowickyj, S.M., Chithalen, J.V., Cameron, D., Tyshenko, M.G., Petkovich, M., Wyatt, G.R., Jones, G., Walker, V.K., 2008. Locust retinoid X receptors: 9-*cis*-retinoic acid in embryos from a primitive insect. Proc. Natl. Acad. Sci. U. S. A. 105, 9540–9545.

Ochoa, W.F., Torrecillas, A., Fita, I., Verdaguer, N., Corbalan-Garcia, S., Gomez-Fernandez, J.C., 2003. Retinoic acid binds to the C2-domain of protein kinase C(alpha). Biochemistry 42, 8774–8779.

Ohta, K., Kawachi, E., Inoue, N., Fukasawa, H., Hashimoto, Y., Itai, A., Kagechika, H., 2000. Retinoidal pyrimidinecarboxylic acids. Unexpected diaza-substituent effects in retinobenzoic acids. Chem. Pharm. Bull. (Tokyo) 48, 1504–1513.

Poon, M.M., Chen, L., 2008. Retinoic acid-gated sequence-specific translational control by RARalpha. Proc. Natl. Acad. Sci. U. S. A. 105, 20303–20308.

Ridgway, R.L., Syed, N.I., Lukowiak, K., Bulloch, A.G., 1991. Nerve growth factor (NGF) induces sprouting of specific neurons of the snail, *Lymnaea stagnalis*. J. Neurobiol. 22, 377–390.

Schrage, K., Koopmans, G., Joosten, E.A., Mey, J., 2006. Macrophages and neurons are targets of retinoic acid signaling after spinal cord contusion injury. Eur. J. Neurosci. 23, 285–295.

Sive, H.L., Draper, B.W., Harland, R.M., Weintraub, H., 1990. Identification of a retinoic acid-sensitive period during primary axis formation in *Xenopus laevis*. Genes Dev. 4, 932–942.

Solomin, L., Johansson, C.B., Zetterstrom, R.H., Bissonnette, R.P., Heyman, R.A., Olson, L., Lendahl, U., Frisen, J., Perlmann, T., 1998. Retinoid-X receptor signalling in the developing spinal cord. Nature 395, 398–402.

Spencer, G.E., Syed, N.I., van Kesteren, E., Lukowiak, K., Geraerts, W.P., van Minnen, J., 2000. Synthesis and functional integration of a neurotransmitter receptor in isolated invertebrate axons. J. Neurobiol. 44, 72–81.

Stratford, T., Horton, C., Maden, M., 1996. Retinoic acid is required for the initiation of outgrowth in the chick limb bud. Curr. Biol. 6, 1124–1133.

Sun, K., Montana, V., Chellappa, K., Brelivet, Y., Moras, D., Maeda, Y., Parpura, V., Paschal, B.M., Sladek, F.M., 2007. Phosphorylation of a conserved serine in the deoxyribonucleic acid binding domain of nuclear receptors alters intracellular localization. Mol. Endocrinol. 21, 1297–1311.

Wiens, M., Batel, R., Korzhev, M., Muller, W.E., 2003. Retinoid X receptor and retinoic acid response in the marine sponge *Suberites domuncula*. J. Exp. Biol. 206, 3261–3271.

Wong, R.G., Hadley, R.D., Kater, S.B., Hauser, G.C., 1981. Neurite outgrowth in molluscan organ and cell cultures: the role of conditioning factor(s). J. Neurosci. 1, 1008–1021.

Wuarin, L., Sidell, N., de Vellis, J., 1990. Retinoids increase perinatal spinal cord neuronal survival and astroglial differentiation. Int. J. Dev. Neurosci. 8, 317–326.

Zhelyaznik, N., Mey, J., 2006. Regulation of retinoic acid receptors alpha, beta and retinoid X receptor alpha after sciatic nerve injury. Neuroscience 141, 1761–1774.